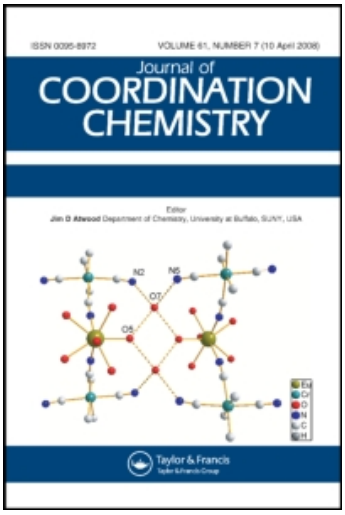

Journal of Coordination Chemistry
Publication details, including instructions for authors and subscription information:
http://www.informaworld.com/smpp/title~content=t713455674

Crystal structure, bioactivities, and electrochemistry properties of four diverse complexes with a new pyrazole ligand

Feilong Hu[a]; Xianhong Yin[a]; Jie Lu[b]; Yan Mi[a]; Jichang Zhuang[a]; Weiqiang Luo[a]
[a] College of Chemistry and Ecological Engineering, Guangxi University for Nationalities, Nanning, China [b] College of Life Science and Technology, Guangxi University, Nanning, China

First published on: 26 October 2009

To cite this Article Hu, Feilong , Yin, Xianhong , Lu, Jie , Mi, Yan , Zhuang, Jichang and Luo, Weiqiang(2010) 'Crystal structure, bioactivities, and electrochemistry properties of four diverse complexes with a new pyrazole ligand', Journal of Coordination Chemistry, 63: 2, 263 — 272, First published on: 26 October 2009 (iFirst)
To link to this Article: DOI: 10.1080/00958970903373930
URL: http://dx.doi.org/10.1080/00958970903373930

Journal of Coordination Chemistry
Vol. 63, No. 2, 20 January 2010, 263–272

Taylor & Francis
Taylor & Francis Group

Crystal structure, bioactivities, and electrochemistry properties of four diverse complexes with a new pyrazole ligand

FEILONG HU†, XIANHONG YIN*†, JIE LU‡, YAN MI†, JICHANG ZHUANG† and WEIQIANG LUO†

†College of Chemistry and Ecological Engineering, Guangxi University for Nationalities, Nanning, China
‡College of Life Science and Technology, Guangxi University, Nanning, China

(*Received 11 May 2009; in final form 24 July 2009*)

Four complexes, $[Cu(cmpa)(Hpdbl)]\cdot 2H_2O$ (**1**), $[Cd(cmpa)_2]\cdot 2.5H_2O$ (**2**), $[Cu(cmpa)_2]\cdot 2.5H_2O$ (**3**), and $[Pb(cmpa)_2]\cdot 2.5H_2O$ (**4**), have been synthesized and characterized based on the pyrazole ligand (Hcmpa = 3-chloro-6-(3,5-dimethy-1-yl)picolinic acid, H_2pdbl = pyridine-2,6-dicarboxylic acid). Complexes **1**–**4** showed 3-D supramolecular architectures that are connected through hydrogen bonds and aromatic π–π interactions. Preliminary antibacterial activities of the complexes indicated selective inhibition for the tested strains. The electrochemistry of **1**–**4** was studied by cyclic voltammetry in DMSO using a glassy carbon working electrode.

Keywords: Pyrazole; Electrochemistry; Crystal structure; Supramolecular

1. Introduction

The design and synthesis of extended frameworks via supramolecular interactions are of interest [1–5]. In particular, hydrogen bonding has been exploited for molecular recognition associated with the biological activity and for engineering of molecular solids. Progress has been made in the construction of organic building blocks into 1-D, 2-D, and 3-D hydrogen bonding architectures. The use of metal complexes as building blocks to assemble multi-dimensional frameworks by hydrogen bonding also attracted recent attention, since the resulting products often exhibit desirable electronic, magnetic, or inclusion behavior.

Pyrazole-derived ligands have been extensively studied [6–10] as monodentate and exobidentate and their nitrogens coordinate as both anionic and neutral groups [11–13]. It is essential to study syntheses and crystal structures of complexes formed by pyrazole systematically to understand the factors that influence the formation and structure of such complexes. Such studies may lead to functional materials and also provide theoretical foundations for supramolecular chemistry and crystal engineering [14]. Carboxylate ligands bind to metal ions to form coordination polymers and are also capable of functioning as hydrogen bond donor or acceptors [15]. Water is important

*Corresponding author. Email: yxhphd@163.com

ISSN 0095-8972 print/ISSN 1029-0389 online © 2010 Taylor & Francis
DOI: 10.1080/00958970903373930

for hydrogen bond networks, especially for the morphologies of water clusters in diverse chemical environments. Water clusters including tetramers [16], hexamers [17], octamers [18], and decamers [19] have been structurally characterized; hydrogen-bonding interaction and their fluctuations are key to the formation of water clusters [20, 21]. We report the coordination of hydroxyl derivatives of picolinic acid toward late 3d-block metals, $[Cu(cmpa)(Hpdbl)] \cdot 2H_2O$ (**1**), $[Cd(cmpa)_2] \cdot 2.5H_2O$ (**2**), $[Cu(cmpa)_2] \cdot 2.5H_2O$ (**3**), and $[Pb(cmpa)_2] \cdot 2.5H_2O$ (**4**).

2. Experimental

2.1. *Materials and analyses*

All reagents and solvents were used directly as supplied commercially, except that Hcmpa was prepared. Elemental analyses (C, H, and N) were determined with a Perkin-Elmer model 240°C automatic instrument. Infrared spectra on KBr pellets were performed on a BRUKER EQUINOX-55 spectrometer from 4000 to 400 cm^{-1}. ^1H NMR spectra were recorded using an INOVA-300 MHZ. Mass spectra were obtained with a JEOL HX-110 HF double focusing spectrometer operating in the positive ion detection mode.

2.2. *Syntheses of the ligand and complexes*

2.2.1. Hcmpa. Hcmpa was prepared by a modified literature method for the preparation of 3-isobutyl-5-pyrazolecarboxylic acid [22].

2.2.2. $[Cu(cmpa)(Hpdbl)] \cdot 2H_2O$ (1). A mixture of Hcmpa (25.1 mg, 0.1 mmol), $CuSO_4 \cdot 5H_2O$ (24.8 mg, 0.1 mmol), 10 mL H_2O, and pyridine-2,6-dicarboxylic acid (H_2pdbl) was sealed in a 25 mL Teflon-lined stainless steel container, which was heated to 150°C for 48 h after cooling to room temperature at a rate of 5°C h^{-1}; well-shaped brown block crystals of **1** suitable for X-ray diffraction were obtained. The crystals were isolated, washed with alcohol three times, and dried in a vacuum desiccator using silica gel (yield 75%). Elemental analysis Calcd (%) for $C_{18}H_{16}ClCuN_4O_8$: C, 41.95; H, 3.13; N, 10.87; O, 24.84; Found (%): C, 41.80; H, 3.15; N, 10.90; O, 24.65.

2.2.3. $[Cd(cmpa)_2] \cdot 2.5H_2O$ (2). A mixture of Hcmpa (25.1 mg, 0.1 mmol), $CdCl_2$ (18.38 mg, 0.1 mmol), and 10 mL water–ethanol (1 : 1) was sealed in a 25 mL Teflon-lined stainless steel container, which was heated to 150°C for 48 h. Slow cooling of the reaction mixture to room temperature gave colorless block crystals in 60% yield. Elemental analysis Calcd (%) for $C_{22}H_{23}CdCl_2N_6O_{6.5}$: C, 40.11; H, 3.52; N, 12.76; O, 15.79; Found (%): C, 40.05; H, 3.56; N, 12.68; O, 15.76.

2.2.4. $[Cu(cmpa)_2] \cdot 2.5H_2O$ (3). A mixture of Hcmpa (25.1 mg, 0.1 mmol), $CuSO4 \cdot 5H_2O$ (24.8 mg, 0.1 mmol), and 10 mL water–ethanol (1 : 1) was sealed in a 25 mL Teflon-lined stainless steel container, which was heated to 150°C for 48 h.

Slow cooling of the reaction mixture to room temperature gave light-yellow block crystals in 60% yield. Anal. Calcd (%) for $CuC_{22}H_{23}Cl_2N_6O_{6.5}$: C, 49.67; H, 4.55; N, 15.80. Found (%): C, 49.62; H, 4.50; N, 15.02.

2.2.5. [Pb(cmpa)$_2$] · 2.5H$_2$O (4). A mixture of Hcmpa (25.1 mg, 0.1 mmol), $PbCl_2$ (27.8 mg, 0.1 mmol), and 10 mL water–ethanol (1 : 1) was sealed in a 25 mL Teflon-lined stainless steel container, which was heated to 150°C for 48 h. Slow cooling of the reaction mixture to room temperature gave light-yellow block crystals in 60% yield. Elemental analysis Calcd (%) for $C_{22}H_{23}Cl_2N_6O_{6.50}Pb$: C, 35.06; H, 3.08; N, 11.15; O, 13.80; Found (%): C, 35.16; H, 3.05; N, 11.05; O, 13.70.

2.3. *X-ray crystallography*

Diffraction experiments for **1**–**4** were carried out with Mo-Kα radiation using a BRUKER SMART APEX CCD diffractometer at 293 K. The structures were solved by direct methods and refined with full-matrix least-squares on F^2 using SHELXS-97 and SHELXL-97 [23]. All non-hydrogen atoms were refined anisotropically. A summary of the crystallographic data and structure refinements is shown in table 1, selected bond lengths and angles of the complexes are listed in table 2, and hydrogen bond geometries are given in table 3.

3. Results and discussion

3.1. *Crystal structures of 1–4*

ORTEP-3 view of the molecular structure of **1** is depicted in figure 1(a) and its crystal structure in figure 2(a). The selected molecular geometry parameters are listed in table 2 and hydrogen bond geometry are listed in table 3.

The copper(II) in **1** is coordinated by one Hcmpa and one H_2pdbl, both bound in a bidentate N,O-chelate, forming two five-membered chelate rings. The geometry around this copper(II) can be described as a distorted octahedral environment. The dihedral angle between the least squares calculated planes through the pyridine ring (N1/C2/C3/C4/C5/C6) and the corresponding six-membered pyridine ring (N4/C13/C14/C15/C16/C17) is 84.0(4)°.

Analysis of the crystal packing of **1** reveals the existence of multiple intermolecular O–H···O hydrogen bonds between mononuclear subunits and lattice water molecules (figure 2a) forming a 2-D, hydrogen-bonded sheet parallel to the (101) plane. In this sheet, the two interstitial water molecules connect three complex molecules, the carboxyl oxygen (O6) which does not coordinate to the Cu(II) center is a hydrogen bond acceptor towards O8 (disordered over two distinct sites with occupancy factors of 0.666 and 0.334, respectively) of one of the water molecules; one of the H atom of O8 in turn binds with the second water molecule, each hydrogen of both water molecules acts as a hydrogen bond donor towards the two carboxyl O2 and O6 of a neighboring complex. The last remaining water H atom (H7f) makes the connection to the third complex connected by the two water molecules (figure 2a). The 2-D sheets are also

Table 1. Crystal data and structure refinements for **1**–**4**.

Complexes	**1**	**2**	**3**	**4**
Empirical formula	$C_{18}H_{17}ClCuN_4O_8$	$C_{22}H_{23}CdCl_2N_6O_{6.50}$	$C_{22}H_{23}Cl_2CuN_6O_{6.50}$	$C_{22}H_{23}Cl_2N_6O_{6.50}Pb$
Formula weight	515.34	658.76	609.90	652.76
Temperature (K)	298(2)	293(2)	298(2)	298(2)
Crystal system	Triclinic	Monoclinic	Monoclinic	Monoclinic
Space group	$P\bar{1}$	$C2/c$	$C2/c$	$C2/c$
Unit cell dimensions (Å, °)				
a	8.4320(10)	20.372(2)	20.192(2)	20.386(2)
b	10.8360(12)	11.5144(13)	11.7740(13)	11.5860(10)
c	11.6110(14)	14.4960(16)	14.3361(15)	14.4680(15)
α	83.5130	90	90	90
β	80.5540(10)	129.511	129.865	129.598
γ	85.871(2)	90	90	90
Volume (Å^3), Z	1038.3(2), 2	2623.4(5), 4	2616.1(5), 4	2633.1(4), 4
Calculated density (g cm^{-3})	1.648	1.668	1.549	1.647
Absorption coefficient (mm^{-1})	1.235	1.087	1.091	0.959
$F(000)$	524	1324	1248	1316
θ range for data collection (°)	1.79–25.00	2.19–19.99	2.17–25.01	2.18–25.00
Data/restraints/parameters	3585/0/330	1220/0/175	2299/0/175	2308/0/185
Goodness-of-fit on F^2	1.093	1.089	1.066	1.099
Final R^a indices [$I > 2\sigma(I)$]	$R_1 = 0.0445$, $wR_2 = 0.1269$	$R_1 = 0.0324$, $wR_2 = 0.0813$	$R_1 = 0.0509$, $wR_2 = 0.1428$	$R_1 = 0.0390$, $wR_2 = 0.113$
R indices (all data)	$R_1 = 0.0580$, $wR_2 = 0.1409$	$R_1 = 0.0370$, $wR_2 = 0.0871$	$R_1 = 0.0708$, $wR_2 = 0.1661$	$R_1 = 0.0511$, $wR_2 = 0.1291$

[a] $R_1 = \Sigma(|F_o| - |F_c|)/\Sigma|F_o|$; $wR_2 = [\Sigma w(|F_o^2| - |F_c^2|)^2/\Sigma w(|F_o^2|^2)]^{1/2}$.

Table 2. Selected bond lengths (Å) and angles (°) for **1**–**4**.

1			
Cu(1)–N(1)	1.932(3)	N(4)–Cu(1)–N(3)	105.57(13)
Cu(1)–O(1)	1.991(3)	N(1)–Cu(1)–O(5)	113.87(13)
Cu(1)–N(4)	2.009(3)	O(1)–Cu(1)–O(5)	93.46(15)
Cu(1)–N(3)	2.044(3)	N(4)–Cu(1)–O(5)	76.11(13)
Cu(1)–O(5)	2.303(3)	N(3)–Cu(1)–O(5)	92.17(14)
Cu(1)–O(3)	2.436(3)	N(1)–Cu(1)–O(3)	96.88(11)
N(1)–Cu(1)–O(1)	80.92(12)	O(1)–Cu(1)–O(3)	91.42(12)
N(1)–Cu(1)–N(4)	169.23(13)	N(4)–Cu(1)–O(3)	73.24(12)
O(1)–Cu(1)–N(4)	94.81(12)	N(3)–Cu(1)–O(3)	93.71(12)
N(1)–Cu(1)–N(3)	78.88(12)	O(5)–Cu(1)–O(3)	149.25(12)
O(1)–Cu(1)–N(3)	159.61(12)		
2			
Cd(1)–O(1)	2.260(4)	N(3)–Cd(1)–N(3)#1	93.3(2)
Cd(1)–N(3)	2.306(5)	O(1)–Cd(1)–N(1)#1	101.31(14)
Cd(1)–N(1)	2.339(4)	O(1)–Cd(1)–N(1)	70.45(15)
O(1)–Cd(1)–O(1)#1	92.3(2)	N(3)–Cd(1)–N(1)#1	120.78(15)
O(1)–Cd(1)–N(3)	137.90(14)	N(3)–Cd(1)–N(1)	68.02(16)
O(1)#1–Cd(1)–N(3)	102.08(16)	N(1)#1–Cd(1)–N(1)	168.5(2)
O(1)–Cd(1)–N(3)#1	102.08(16)	O(1)#1–Cd(1)–N(1)	101.31(14)
N(3)#1–Cd(1)–N(1)	120.78(15)		
3			
Cu(1)–N(1)	2.076(3)	N(1)–Cu(1)–O(1)	76.55(12)
Cu(1)–O(1)	2.096(3)	O(1)#2–Cu(1)–O(1)	93.4(2)
Cu(1)–N(3)	2.134(4)	N(1)#2–Cu(1)–N(3)#2	74.41(13)
N(1)#2–Cu(1)–N(1)	167.5(2)	N(1)–Cu(1)–N(3)#2	115.10(13)
N(1)#2–Cu(1)–O(1)#2	76.55(12)	O(1)#2–Cu(1)–N(3)#2	149.96(12)
4			
Pb(1)–O(1)	2.241(3)	O(1)–Pb(1)–N(1)#3	100.85(12)
Pb(1)–N(3)	2.279(4)	N(3)#3–Pb(1)–N(1)#3	68.86(12)
Pb(1)–N(1)	2.303(3)	N(3)–Pb(1)–N(1)#3	119.65(12)
O(1)#3–Pb(1)–O(1)	92.2(2)	O(1)#3–Pb(1)–N(1)	100.85(12)
O(1)–Pb(1)–N(3)#3	101.37(13)	O(1)–Pb(1)–N(1)	71.16(12)
O(1)#3–Pb(1)–N(3)	101.37(13)	N(3)#3–Pb(1)–N(1)	119.65(12)
O(1)–Pb(1)–N(3)	139.48(12)	N(3)–Pb(1)–N(1)	68.86(12)
N(3)#3–Pb(1)–N(3)	92.70(19)	N(1)#3–Pb(1)–N(1)	168.86(17)

Symmetry transformations used to generate equivalent atoms. #1: $-x+1$, y, $-z+1/2$, #2: $-x+1$, y, $-z+1/2$, #3: $-x+2$, y, $-z+3/2$.

assembled in the (101) direction by $\pi\cdots\pi$ stacking interaction [24] between the pyridine rings defined by atoms N1/C2/C3/C4/C5/C6 (centroid–centroid distance 3.636 Å, dihedral angle 0°). There is one more $\pi\cdots\pi$ stacking interaction between the pyridine rings defined by atoms N4/C13/C14/C15/C16/C17 (centroid–centroid distance 3.600 Å, dihedral angle 0°) as viewed from figure 3(a). ORTEP-3 view of the molecular structure of **2** is depicted in figure 1(b) and its crystal structure in figure 2(b). The selected molecular geometry parameters are listed in table 2 and hydrogen bond geometry in table 3.

Cadmium(II) in **2** is six-coordinate with four nitrogens and two oxygens derived from the tridentate Hcmpa in a distorted octahedral environment. In the crystal structure, the oxygens form intermolecular hydrogen bonds involving the solvate waters, two waters, and Hcmpa via intermolecular O–H$\cdots$O hydrogen bonds. A great number of hydrogen contacts link the complex into a 3-D network (figure 2b). The $\pi\cdots\pi$ stacking interaction between the pyridine rings also contribute to the formation of the structure with the centroid–centroid distance 3.5544(3) Å (figure 3b). The dihedral angle between

Table 3. Hydrogen-bonding geometries for **1**–**4**.

D–H···A	Symmetry code	D–H (Å)	H···A (Å)	D···A (Å)	D–H···A (°)
1					
O7–H7F···O6_a		0.850	1.725	2.574	176.09
O7–H7F···O6′_b		0.850	2.125	2.877	147.21
O7–H7G···O2	$x+1, y, z$	0.850	1.878	2.726	175.86
O8–H8C_a···O7	$x, y, z-1$	0.850	2.230	3.042	159.69
O8–H8D_a···O7	$-x+1, -y+2, -z+1$	0.850	1.881	2.688	157.98
O8′–H8′C_b···O5		0.850	2.277	2.957	137.09
O8′–H8′D_b···O6′_b		0.850	1.861	2.545	136.40
2					
O3–H3A···O2	$x, y, z+1$	0.850	2.184	3.033	176.57
O3–H3B···O2	$-x+1, y, -z+1$	0.850	2.025	2.873	175.78
O4–H4A···O3	$-x+1, -y+1, -z+1$	0.850	1.607	2.456	176.69
3					
O3–H3A···O2	$x, y-1, z$	0.850	1.966	2.810	171.60
O3–H3B···O2	$-x+1, -y+1, -z$	0.850	2.068	2.912	171.93
O4–H4···O3		0.850	1.759	2.609	178.69
4					
O3–H3A···O2′_b	$-x+3/2, y+1/2, -z+3/2$	0.850	1.965	2.803	168.83
O3–H3A···O2_a	$-x+3/2, y+1/2, -z+3/2$	0.850	2.117	2.964	174.65
O3–H3B···O2_a	$x-1/2, -y+1/2, z-1/2$	0.850	1.947	2.796	175.65
O3–H3B···O2′_b	$x-1/2, -y+1/2, z-1/2$	0.850	2.294	3.125	165.76
O4–H4A···O3		0.850	1.742	2.592	179.21

Oxygen atoms of some water molecules are divided into part a and b due to disorder.

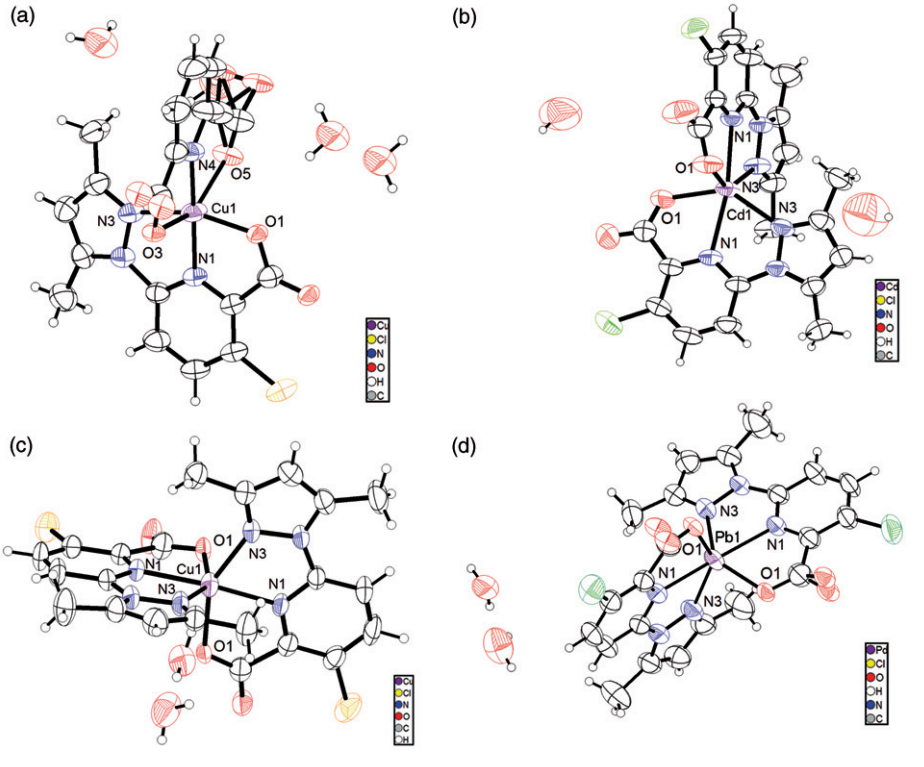

Figure 1. The coordinate geometry of **1**–**4**.

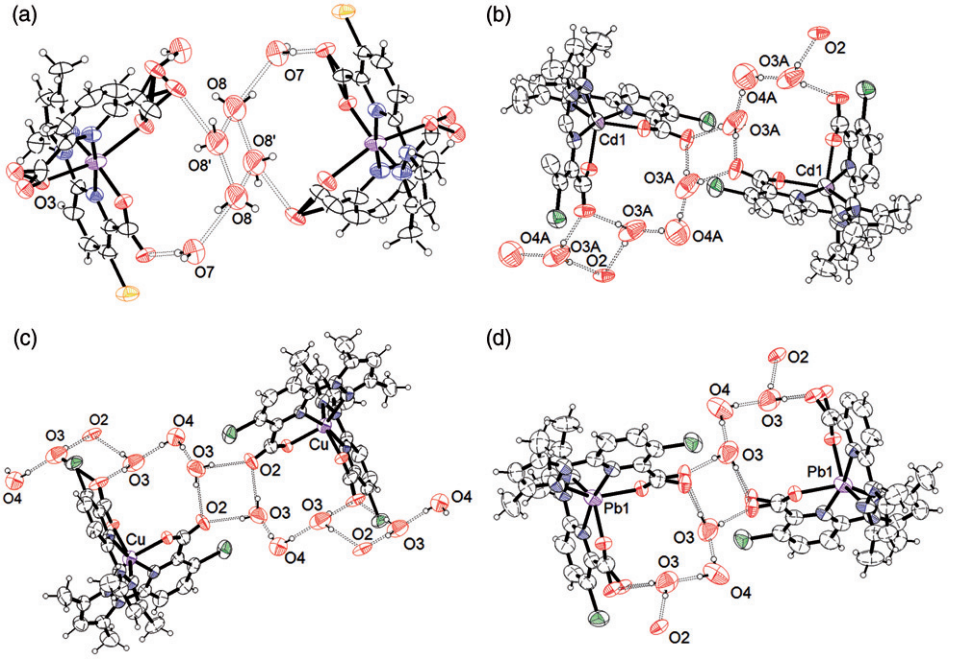

Figure 2. A view of the crystal packing of **1**–**4** showing the O–H···O hydrogen bonds. Displacement ellipsoids are drawn at the 50% probability level and the hydrogen bonds are indicated by dashed lines.

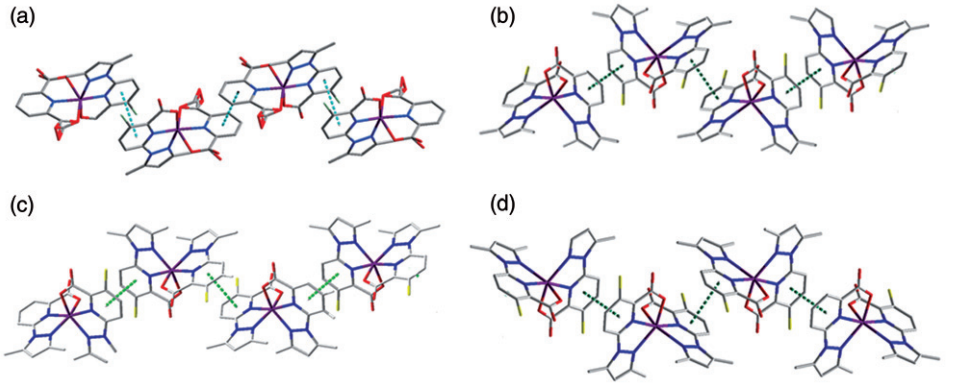

Figure 3. The $\pi \cdots \pi$ stacking interactions of **1**–**4**.

the least squares planes through the pyridine ring (N1/C2/C3/C4/C5/C6) and the corresponding five-membered chelate ring (Cd1/N1/N2/N3/C6) is 1.98°.

ORTEP-3 views of the molecular structures of **3** and **4** are depicted in figure 1(c) and (d). The selected molecular geometry parameters are listed in table 2 and hydrogen bond geometry in table 3.

The coordination environment in **3** and **4** is similar to **2** with both Cu and Pb six coordinate by four oxygens and two nitrogens.

The crystal packing of **3** and **4** reveals the existence of multiple intermolecular O–H···O hydrogen bonds between the mononuclear subunits and the lattice water

Table 4. Characteristic IR bands (cm^{-1}) of the ligands and their complexes.

Compounds	ν(O–H)	ν(C=O)	ν(C=N)	ν(C–N)	ν(M–O)	ν(M–N)
HCMPA	3440	1730	1565	1234		
Cu(cmpa)(pdbl) · $2H_2O$	3385	1706	1545	1225	422	520
$Cd(cmpa)_2 \cdot 2H_2O$	3438	1647	1533	1247	422	503
$Cu(cmpa)_2 \cdot 2H_2O$	3365	1688	1529	1226	418	507
$Pb(cmpa)_2 \cdot 2H_2O$	3487	1675	1526	1250	415	506

molecules (figure 2c and d), forming a 3-D hydrogen bonded sheet perpendicular to the *c*-axis of the structure. In the sheet two interstitial water molecules connect three complexes with each other. The O4 of one water molecule is a double hydrogen donor toward O3, and each hydrogen of O3 is a hydrogen bond donor towards the two carboxyl oxygens O2 and its symmetry equivalent of a neighboring complex, leading to a 3-D supramolecular structure. The carboxylate that is a hydrogen acceptor towards both waters via O1 and O2 exhibits a delocalized π system with nearly identical C–O distances. Also, the $\pi \cdots \pi$ stacking interaction between the pyridine rings contribute to the formation of the structure with the centroid–centroid distance 3.599 Å for **3** and 3.557 Å for **4** (figure 3c and d).

3.2. *Vibrational spectroscopy*

The IR spectra of all four complexes are similar, indicating similar structures. Table 4 summarizes the characteristic bands observed for the ligand and its metal complexes. The IR spectrum of the free ligand shows strong bands at 1730 and 1565 cm^{-1}, which can be assigned as ν(C=O) and ν(C=N), respectively. In the complexes, these bands shift upfield by 24–83 cm^{-1} for ν(C=O) and 20–39 cm^{-1} for ν(C=N). In each case, the shift suggests that the relevant oxygen and nitrogen of the ligand coordinated to the metal [25]. The bands centered at 3365–3487 cm^{-1} can be attributed to lattice water molecules in agreement with the crystal structures of the complexes. The absorption bands assigned to the M–O and M–N stretching frequencies of the complexes were observed at 550–590 cm^{-1} and 423–435 cm^{-1}, respectively [26–28].

These results indicate that the ligands coordinate to metal via oxygen of the carboxyl and nitrogen of the pyridine or pyrazole.

3.3. *Electrochemistry*

The cyclic voltammetric measurement of **1** and **3** was carried out in dimethylsulfoxide at 25°C under a nitrogen atmosphere using glassy carbon as the working electrode and at a scan rate of 100 mV s^{-1}. The cyclic voltammograms of **1** and **3** are shown in figure 4. In the potential range of 1 to −1.5 V, **3** displays one couple of oxidation/reduction peaks (figure 4a), which corresponds to Cu(II)/Cu(I) [29–32]. Electric potentials of cathode and anode are $E_{pc} = -0.118$ V and $E_{pa} = 0.024$ V with $E_{1/2} = -0.047$ V. From ΔE (−0.142 V) and I_{pc}/I_{pa} (0.92), the electron transfer is quasi-reversible. Complex **1** displays quasi-reversible reaction with one couple of oxidation/reduction peaks in the potential range of 0.4 to −0.6 V (figure 4b), which corresponds to Cu(II)/Cu(I); electric

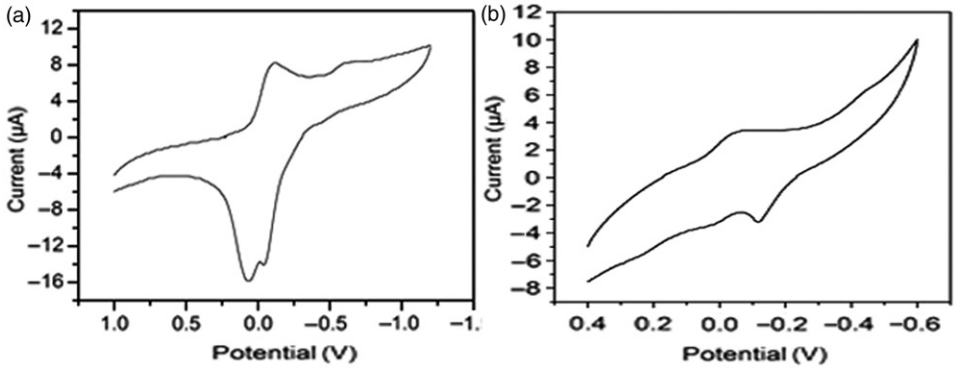

Figure 4. Cyclic voltammograms of **1** and **3**, scan rate ($100\,mv\,s^{-1}$).

Table 5. Zones of inhibitions of pyrazole complexes against five different bacteria.

Compound	*Bacillus* WD	*Staphylococcus* WD	*Escherichia* WD	*Salmonella* WD	Yeast WD
$Cu(cmpa)(pdbl)\cdot 2H_2O$	+	+++	+++	+++	+++
$Cd(cmpa)_2\cdot 2H_2O$	+++	+++	+++	+	+++
$Cu(cmpa)_2\cdot 2H_2O$	++	+++	+++	+++	+++
$Pb(cmpa)_2\cdot 2H_2O$	++	+++	+++	+++	+++
0	–	–	–	–	–
N	–	–	–	–	–

MIC: minimum inhibitory concentration; +++: bacterial appearance time longer than 40 h (strong activity); ++: bacterial appearance time longer than 32 h (middle strong activity); +: bacterial appearance time longer than 22 h (common activity); –: bacterial appearance time shorter than 22 h (no activity); 0: water blank without bacterium; N: solvent blank.

potentials of cathode and anode are $E_{pc} = -0.6479\,V$ and $E_{pa} = -0.1214\,V$ with $E_{1/2} = -0.3846\,V$. Due to the electron-withdrawing nature of the chloro substituent, **3** displays an anodic shift.

3.4. *Antibacterial activity*

The antibacterial activity of pyrazole complexes were tested against *Bacillus*, *Staphylococcus*, *Escherichia*, *Salmonella*, and Yeast. The microdilution broth method was used to determine the antibacterial activity (table 5) [33]. The ligand and complexes possess a broad spectrum of activity against the tested bacteria at MIC values between 76 and $660\,\mu g\,mL^{-1}$ with Pb(II) and Cd(II) complexes more active than Cu(II) complexes.

Supplementary material

Crystallographic data (excluding structure factors) for the structure in this article have been deposited with the Cambridge Crystallographic Data Centre as supplementary

publications CCDC 721369-721372 for **1**–**4**, respectively. Copies of the data can be obtained free of charge on application to CCDC, 12 Union Road, Cambridge CB2 1EZ, UK (Fax: 441223-336-033; Email: deposit@ccdc.cam.ac.uk).

Acknowledgments

The authors thank the National Natural Science Foundation of China (20761002), P.R. China, and the Natural Science Foundation of GuangXi (0832080).

References

[1] B. Moulton, M.J. Zaworotko. *Chem. Rev.*, **101**, 1629 (2001).
[2] A.Y. Robin, K.M. Fromm. *Coord. Chem. Rev.*, **250**, 2127 (2006).
[3] J.J. Vittal. *Coord. Chem. Rev.*, **251**, 1781 (2007).
[4] R. Horikoshi, T. Mochida. *Coord. Chem. Rev.*, **250**, 2595 (2006).
[5] N.R. Champness. *Dalton Trans.*, 877 (2006).
[6] R. Mukherjee. *Coord. Chem. Rev.*, **203**, 151 (2000).
[7] F.L. Hu, X.H. Yin, Y. Mi, J.L. Zhang, Y. Zhuang, X.Z. Dai. *Inorg. Chem. Commun.*, **12**, 628 (2009).
[8] U.N. Tripathi, J. Solanki, M.S. Ahmad, A. Bhardwaj. *J. Coord. Chem.*, **62**, 636 (2009).
[9] Q.J. Zhou, Y.Z. Liu, R.L. Wang, J.W. Fu, J.Y. Xu, J.S. Lou. *J. Coord. Chem.*, **62**, 311 (2009).
[10] B. Zhao, H.M. Shu, H.M. Hu, T. Qin, X.L. Chen. *J. Coord. Chem.*, **62**, 1025 (2009).
[11] A.P. Martinez, M.J. Fabra, M.P. García, F.J. Lahoz, L.A. Oro, S.J. Teat. *Inorg. Chim. Acta*, **358**, 1635 (2005).
[12] G. La Monica, G.A. Ardizzoia. *Prog. Inorg. Chem.*, **46**, 151 (1997).
[13] S. Trofimenko. *Chem. Rev.*, **93**, 943 (1993).
[14] (a) J.D. Woodward, R.V. Backov, K.A. Abboud, D.R. Talham. *Polyhedron*, **25**, 2605 (2006); (b) Z.F. Tian, Y. Su, J.G. Lin, Q.J. Meng. *Polyhedron*, **26**, 2829 (2007); (c) Z.G. Guo, X.J. Li, S.Y. Gao, Y.F. Li, R. Cao. *J. Mol. Struct.*, **846**, 123 (2007).
[15] C.N.R. Rao, S. Natarajan, R. Vaidhyanathan. *Angew. Chem. Int. Ed.*, **43**, 1466 (2004).
[16] B.H. Ye, A.P. Sun, T.F. Wu, Y.Q. Weng, X.M. Chen. *Eur. J. Inorg. Chem.*, 1230 (2005).
[17] B.H. Ye, B.B. Ding, Y.Q. Weng, X.M. Chen. *Inorg. Chem.*, **43**, 6866 (2004).
[18] J.L. Atwood, L.J. Barbour, T.J. Ness, C.L. Raston, P.L. Raston. *J. Am. Chem. Soc.*, **123**, 7192 (2001).
[19] L.J. Barbour, G.W. Orr, J.L. Atwood. *Nature*, **393**, 671 (1998).
[20] (a) J. Kim, K.S. Kim. *Chem. Phys.*, **109**, 5886 (1996); (b) J. Yang, J.F. Ma, Y.Y. Liu, J.C. Ma, H.Q. Jia, N.H. Hu. *Eur. J. Inorg. Chem.*, 1208 (2006).
[21] (a) P. Rodríguez-Cuamatzi, G. Vargas-Díaz, H. Höpfl. *Angew. Chem. Int. Ed.*, **43**, 3041 (2004); (b) B.Q. Ma, H.L. Sun, S. Gao. *Angew. Chem. Int. Ed.*, **43**, 1374 (2004).
[22] G.B. Pier, C. Baarfara, R. Romeo, S. Giampiero. *Synthesis*, **3**, 453 (1999).
[23] G.M. Sheldrick. *SHELXL97 and SHELXTL Software Reference Manual*, Vol. 5.1, Bruker AXS Inc., Madison, WI, USA (1997).
[24] C. Janiak. *J. Chem. Soc., Dalton Trans.*, 3885 (2000).
[25] R. March, W. Clegg, R.A. Coxall, L. Cucurull-Sánchez, L. Lezama, T. Rojo, P. González-Duarte. *Inorg. Chim. Acta*, **353**, 129 (2003).
[26] J.R. During, R. Layton, D.N. Sink, B.R. Mitchell. *Spectrochim. Acta*, **21**, 1326 (1965).
[27] K. Ueno, A.E. Martell. *J. Phys. Chem.*, **60**, 1270 (1956).
[28] G. Percy. *Spectrochim. Acta*, **32A**, 1287 (1976).
[29] M. Thirumavalavan, P. Akilan, M. Kandaswamy, K. Chinnakali, G.S. Kumar, H.K. Fun. *Inorg. Chem.*, **42**, 3308 (2003).
[30] R.J. Crutchley, R. Hynes, E.J. Gabe. *Inorg. Chem.*, **29**, 4921 (1990).
[31] J. Casanova, G. Alzuet, J. Latorre, J. Borrás. *Inorg. Chem.*, **36**, 2052 (1997).
[32] A. Widmann, H. Kahlert, I. Petrovic-Prelevic, H. Wulff, J.V. Yakhmi, N. Bagkar, F. Scholz. *Inorg. Chem.*, **41**, 5706 (2002).
[33] Y.M. Al-Hiari, B.A. Sweileh. *Asian J. Chem.*, **18**, 2285 (2006).